MOLECULAR AND CELLULAR BIOLOGY, Dec. 2011, p. 4706–4719 Vol. 31, No. 23
0270-7306/11/$12.00 doi:10.1128/MCB.05980-11

Biphasic and Dosage-Dependent Regulation of Osteoclastogenesis by β-Catenin▽

Wei Wei,[1]† Daniel Zeve,[2]† Jae Myoung Suh,[2] Xueqian Wang,[1] Yang Du,[1] Joseph E. Zerwekh,[4,5] Paul C. Dechow,[6] Jonathan M. Graff,[2,3,4] and Yihong Wan[1]*

Department of Pharmacology,[1] Department of Developmental Biology,[2] Department of Molecular Biology,[3] Department of Internal Medicine,[4] and Center for Mineral Metabolism and Clinical Research,[5] University of Texas Southwestern Medical Center, Dallas, Texas 75390, and Department of Biomedical Sciences, Baylor College of Dentistry, Texas A&M University Health Sciences Center, Dallas, Texas 75246[6]

Received 21 July 2011/Accepted 20 August 2011

Wnt/β-catenin signaling is a critical regulator of skeletal physiology. However, previous studies have mainly focused on its roles in osteoblasts, while its specific function in osteoclasts is unknown. This is a clinically important question because neutralizing antibodies against Wnt antagonists are promising new drugs for bone diseases. Here, we show that in osteoclastogenesis, β-catenin is induced during the macrophage colony-stimulating factor (M-CSF)-mediated quiescence-to-proliferation switch but suppressed during the RANKL-mediated proliferation-to-differentiation switch. Genetically, β-catenin deletion blocks osteoclast precursor proliferation, while β-catenin constitutive activation sustains proliferation but prevents osteoclast differentiation, both causing osteopetrosis. In contrast, β-catenin heterozygosity enhances osteoclast differentiation, causing osteoporosis. Biochemically, Wnt activation attenuates whereas Wnt inhibition stimulates osteoclastogenesis. Mechanistically, β-catenin activation increases GATA2/Evi1 expression but abolishes RANKL-induced c-Jun phosphorylation. Therefore, β-catenin exerts a pivotal biphasic and dosage-dependent regulation of osteoclastogenesis. Importantly, these findings suggest that Wnt activation is a more effective treatment for skeletal fragility than previously recognized that confers dual anabolic and anti-catabolic benefits.

Skeletal homeostasis is mainly regulated by bone-resorbing osteoclasts and bone-forming osteoblasts. Osteoclasts derive from hematopoietic progenitors (1), while osteoblasts derive from mesenchymal progenitors (26). During osteoclastogenesis, osteoclast progenitors undergo a quiescence-to-proliferation switch in response to macrophage colony-stimulating factor (M-CSF), and then osteoclast precursors undergo a proliferation-to-differentiation switch in response to receptor activator of NF-κB ligand (RANKL) (18, 40). Defects in osteoclast function may cause osteopetrosis (34). In contrast, pathological stimulation of osteoclast activities occurs in osteoporosis (14a, 14b, 17a), arthritis (13, 17), and bone metastasis of cancers (20a, 28a). Thus, osteoclasts are critical for bone remodeling, but their activity must be controlled (22, 34).

β-Catenin is an essential component transducing canonical Wnt signaling. Wnt activation results in inhibition of glycogen synthase kinase 3β (GSK-3β)-mediated β-catenin phosphorylation and thereby stabilization of β-catenin protein (20). The Wnt/β-catenin pathway is an important regulator of skeletal physiology. β-Catenin deletion in mesenchymal progenitors blocks osteoblast differentiation by shifting to chondrocyte formation (8, 13a). β-Catenin deletion in differentiated osteoblasts leads to osteopenia by reducing the expression of osteoprotegerin (OPG), a decoy RANKL receptor, thus indirectly elevating osteoclast formation (11, 14). Furthermore, Wnt/β-catenin activation enhances osteoblastogenesis and suppresses adipogenesis by inhibiting peroxisome proliferator-activated receptor γ (PPARγ) (2a, 14d). Therefore, β-catenin is required for osteoblast differentiation and modulates osteoblast function.

Despite the intense investigation of Wnt/β-catenin signaling in bone biology, previous studies have mainly focused on its roles in osteoblasts, while its specific functions, if any, in osteoclasts are unknown. This is a clinically important question because Wnt-activating drugs are currently in trials as new treatment for bone diseases (9, 10, 19, 23, 27, 33). Emerging evidence revealed that PPARγ is an important regulator of osteoclast lineage commitment and differentiation: on one hand, PPARγ is highly expressed in both osteoclast precursors and mature osteoclasts (28, 35, 37), and PPARγ deletion causes osteoclast defects manifested as osteopetrosis (37); on the other hand, activation of PPARγ by the diabetic drug rosiglitazone (BRL, or Avandia) stimulates osteoclast differentiation and bone resorption (18a, 37, 38, 42). Moreover, our recent study shows that PPARγ is also expressed in osteoclast progenitors: PPARγ-tTA TRE-H2BGFP reporter mice (31) label the entire osteoclast lineage, from osteoclast progenitors to mature osteoclasts, as a green fluorescent protein-positive (GFP^+) hematopoietic bone marrow cell population; as a complement, PPARγ-tTA TRE-Cre mice enable genetic manipulation in the osteoclast progenitors and the entire osteoclast lineage in a spatially and temporally controllable manner (38a). In light of the mutual inhibition between Wnt and PPARγ in the mesenchymal lineages (30), here, we ask whether and how Wnt/β-catenin signaling also regulates osteoclastogenesis.

* Corresponding author. Mailing address: Department of Pharmacology, UT Southwestern Medical Center, 6001 Forest Park Road, Room ND8.502B, Dallas, TX 75390-9041. Phone: (214) 645-6062. Fax: (214) 645-6166. E-mail: yihong.wan@utsouthwestern.edu.
† W.W. and D.Z. contributed equally to this study.
▽ Published ahead of print on 29 August 2011.

MATERIALS AND METHODS

Mice. PPARγ-tTA TRE-H2BGFP mice (31), Catnb$^{+/lox(ex3)}$ mice (12), β-catenin$^{fl/fl}$ mice (4), Tie2-cre mice (7, 16, 37), LyM-cre mice (6), and Ctsk (cathepsin K)-cre mice (21) have been described previously. PPARγ-tTA TRE-cre mice were bred with Catnb$^{+/lox(ex3)}$ mice to generate PTbCA mice. PPARγ-tTA TRE-cre mice were bred with β-catenin$^{fl/fl}$ mice to generate PTbKO and PTbHet mice. All experiments were performed using littermate cohorts. All protocols for mouse experiments were approved by the Institutional Animal Care and Use Committee of the University of Texas Southwestern Medical Center.

Bone analyses. To evaluate bone volume and architecture by micro-computed tomography (μCT), mouse tibiae were fixed in 70% ethanol. The tibiae were scanned using a Scanco μCT-35 instrument (Scanco Medical) at several resolutions for both overall tibial assessment (14-μm resolution) and structural analysis of trabecular and cortical bone (7-μm resolution). Trabecular bone parameters were calculated using Scanco software to analyze the bone scans from the trabecular region directly distal to the proximal tibial growth plate. Static histomorphometric analyses were conducted using Bioquant Image Analysis software (Bioquant). Dynamic histomorphometric analyses were performed as previously described (37), and calcein (20 mg/kg of body weight) was injected into 2-month-old mice 2 and 10 days before bone collection. TRAP (tartrate-resistant acid phosphatase) staining of osteoclasts was performed using a leukocyte acid phosphatase staining kit (Sigma). ALP staining of osteoblasts was performed using an alkaline phosphatase staining kit (Sigma). As a bone resorption marker, urinary or serum C-terminal telopeptide fragments of the type I collagen (CTX-1) was measured with the RatLaps enzyme immunoassay (EIA) kit (Immunodiagnostic Systems). Urinary CTX-1 was normalized by urinary creatinine measured with the Infinity Creatinine Reagent (Thermo Scientific). As a bone formation marker, serum osteocalcin was measured with the mouse osteocalcin EIA kit (Biomedical Technologies Inc.).

***In vitro* osteoclast differentiation.** Osteoclasts were differentiated from mouse bone marrow cells as described previously (15, 37, 38). Briefly, hematopoietic bone marrow cells were purified with a 40-μm cell strainer to remove mesenchymal cells and differentiated with 40 ng/ml of M-CSF in α minimal essential medium (α-MEM) containing 10% fetal bovine serum (FBS) for 3 days and then with 40 ng/ml of M-CSF and 100 ng/ml of RANKL for 3 days (unless otherwise stated) in the presence or absence of BRL (1 μM). Mature osteoclasts were identified as multinucleated (>3 nuclei) TRAP$^+$ cells. Osteoclast differentiation was quantified by the RNA expression of RANKL-induced transcription factors and osteoclast function genes using reverse transcription-quantitative PCR (RT-QPCR) analysis. Protein expression or phosphorylation was analyzed by Western blotting. The following reagents were used: recombinant mouse M-CSF, RANKL, and Wnt3A (R&D Systems) and the GSK3β inhibitor 6-bromoindirubin-3′-oxime (BIO) and the inactive control metBIO (Calbiochem). The following antibodies were used: anti-β-catenin and anti-cyclin D1 (BD Biosciences), anti-c-jun and anti-phospho-c-jun (Cell Signaling), anti-IκBα (Santa Cruz), and anti-β-actin (Sigma).

Osteoclast precursor proliferation assay. Osteoclast precursor proliferation was quantified using a bromodeoxyuridine (BrdU) cell proliferation assay kit (GE Healthcare Life Sciences) (2). Mouse bone marrow cells were treated with M-CSF (40 ng/ml) for 3 days. On day 4, the cells were M-CSF starved for 6 h and then restimulated with M-CSF for 4 h to induce S phase, during which BrdU was provided in the culture medium. Cell proliferation was quantified as BrdU incorporation using the BrdU enzyme-linked immunosorbent assay (ELISA) in the kit.

Gene expression analyses. RNA was reverse transcribed into cDNA using an ABI High Capacity cDNA RT Kit and analyzed using real-time quantitative PCR (SYBR green) in triplicate. All RNA expression was normalized by ribosomal protein L19.

Flow cytometry. The fluorescence-activated cell sorter (FACS) analyses of bone marrow cells were performed using a BD FACScan flow cytometer and phycoerythrin (PE)-conjugated antibody against c-Kit (BD Pharmingen).

Transfection. Bone marrow cells were purified with a 40-μm cell strainer to remove mesenchymal cells and cultured with 40 ng/ml M-CSF overnight. Cells in suspension were removed, and adherent osteoclast progenitors/precursors were transfected using FuGene HD (Roche) in the presence of 40 ng/ml M-CSF, with cDNA-expressing plasmid (or vector control), or with small interfering RNA (siRNA) (or control) for 3 days before RANKL-induced osteoclast differentiation. Expression plasmids encoding wild-type (WT) c-Jun or the c-Jun$^{Ser63/73Asp}$ mutant (JunS63/73D) were generous gifts from D. Bohmann (3, 25). Expression plasmids encoding WT or constitutively active β-catenin were generous gifts from C. Zhang (41). mGATA2 siRNA, mEvi1 siRNA, and control siRNA were from Santa Cruz.

Statistical analyses. All statistical analyses were performed with Student's *t* test and represented as means and standard deviations (SD). The *P* values were designated as follows: *, $P < 0.05$; **, $P < 0.01$; ***, $P < 0.005$; ****, $P < 0.001$; *****, $P < 0.0005$; ****** (or ^), $P < 0.0001$; NS, nonsignificant ($P > 0.05$).

RESULTS

β-Catenin constitutive activation in the osteoclast lineage causes osteopetrosis. To unravel the functions of canonical Wnt signaling in osteoclastogenesis, we focused our attention on β-catenin, because it is an obligatory and nonredundant downstream component of a diverse array of Wnt ligands and receptors. To establish mouse genetic models harboring β-catenin mutations in the osteoclast lineage, we employed several Cre drivers, including Tie2-cre for hemagioblast stem cell targeting (7, 37), PPARγ-tTA TRE-cre for osteoclast progenitor targeting (38a), lysozyme (Lyz)-cre for macrophage precursor targeting (6), and Ctsk-cre for preosteoclast and mature osteoclast targeting (21). Because of its ability to target β-catenin in osteoclast progenitors without causing embryonic lethality, we focused our studies on the PPARγ driver.

To determine the effects of β-catenin activation on osteoclastogenesis, we generated a mouse model harboring an inducible β-catenin gain-of-function mutation in PPARγ$^+$ cells. Mice expressing a conditional β-catenin mutant allele in which exon 3, which encodes all the serine and threonine residues phosphorylated by GSK-3β, is flanked by *loxP* sequences have been previously generated (Catnb$^{+/lox(ex3)}$) (12). Cre-mediated deletion of exon 3 prevents β-catenin phosphorylation by GSK-3β and its subsequent degradation, thereby creating a constitutively active molecule (20). We bred Catnb$^{+/lox(ex3)}$ mice with PPARγ-tTA TRE-cre mice to generate PTbCA (PPARγ-tTA TRE-cre-mediated β-catenin constitutive activation) mice (Fig. 1A). The PTbCA mice were compared with the PPARγ-tTA TRE-cre controls (PTctrl). Importantly, this system conferred a Tet-off temporal control of β-catenin activation. In the absence of doxycycline (Dox), the PTbCA mice expressed the bCA mutant allele in all the PPARγ$^+$ cells. When tTA activity was inhibited by Dox from embryonic day 0 (E0), the bCA mutant allele was not activated until Dox was removed (Fig. 1A).

A series of analyses revealed that the PTbCA mutants exhibited severe osteopetrosis. Strikingly, μCT imaging of the tibiae from 10-month-old mice showed that the trabecular bone volume/tissue volume (BV/TV) ratio was increased by 27-fold compared to the controls (Fig. 1B and C). Consistently, the trabecular bones exhibited a greater bone surface (BS) (+4.6-fold), trabecular number (Tb.N.) (+3.6-fold), and trabecular thickness (Tb.Th.) (+8.5-fold), accompanied by a smaller bone surface/bone volume (BS/BV) ratio (−86%) and trabecular separation (Tb.Sp.) (−97%) (Fig. 1C). The BV/TV ratio of the cortical bone and the whole tibia was also significantly elevated (Fig. 1C). These results indicate that β-catenin constitutive activation in the osteoclast lineage causes severely increased bone mass and a highly diminished marrow cavity.

μCT analysis of 15-day-old pups showed that this bone phenotype had already developed at postnatal day 15 (P15) (http://www4.utsouthwestern.edu/wanlab/publications.htm). The BV/TV ratio was significantly increased in the trabecular

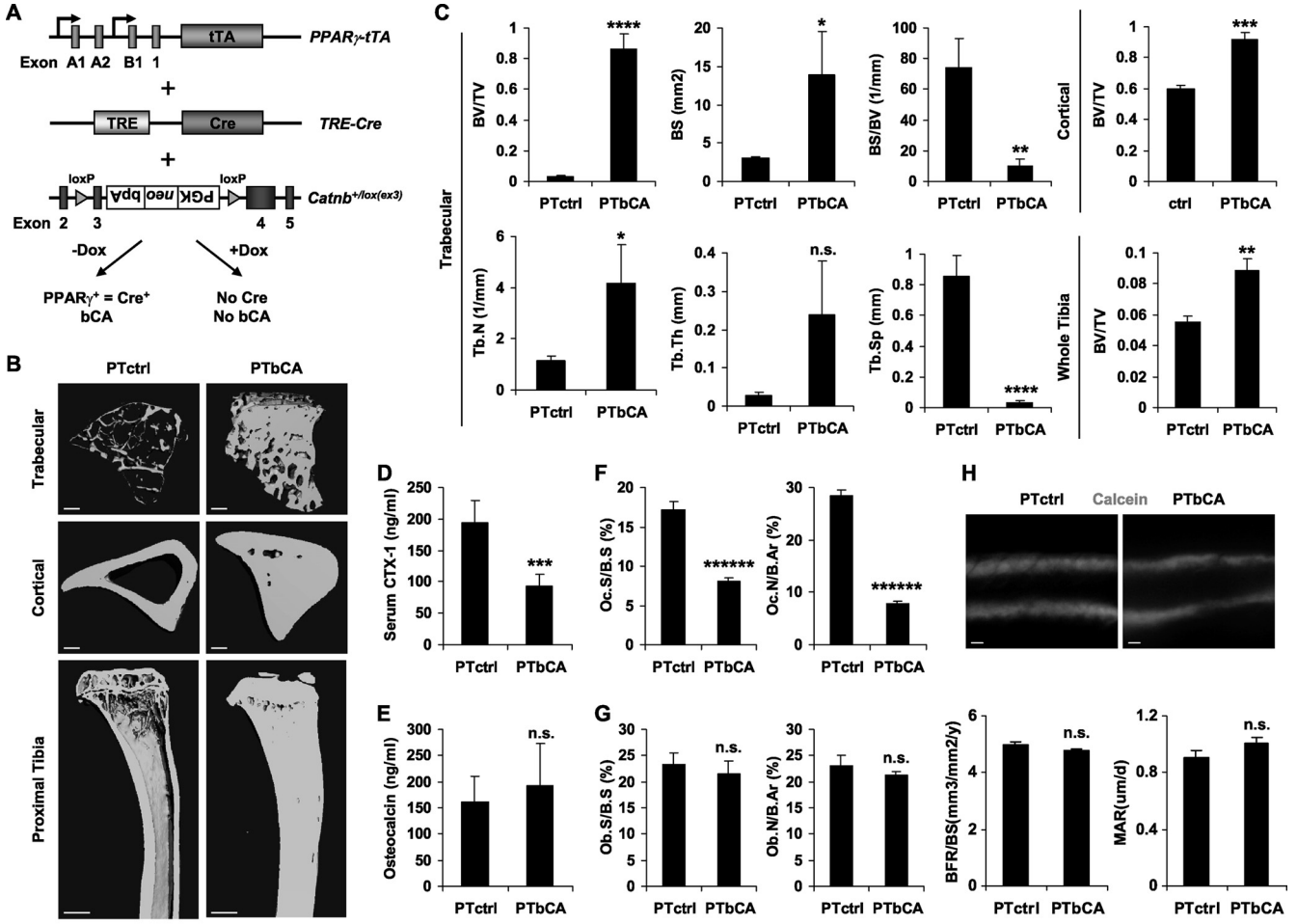

I

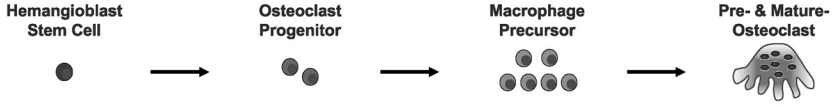

	Tie2-bCA (lethal)	PTbCA	Lyz-bCA	Ctsk-bCA
BV/TV	N.D.	+1658%	+499%	+247%
CTX-1	N.D.	-79%	-34%	-18%
Osteocalcin	N.D.	-6%	N.C.	N.C.
OcN/Well	N.D.	-96%	-71%	-48%

N.D, not determined; N.C., no significant change.

FIG. 1. β-Catenin constitutive activation in the osteoclast lineage causes osteopetrosis. (A) Schematic diagram of PPARγ-tTA TRE-cre Catnb$^{+/lox(ex3)}$ (PTbCA) mice. bCA, β-catenin constitutively activated. (B and C) μCT analysis of the tibiae from PTbCA or control (PTctrl) mice (10 months old; male; $n = 3$). (B) Representative μCT images of the trabecular and cortical bones (scale bars, 10 μm) and the entire proximal tibia (scale bars, 1 mm). (C) Quantification of tibial parameters. The error bars indicate SD. (D) Serum CTX-1 was significantly decreased in PTbCA mice (15 days old; $n = 7$). (E) Serum osteocalcin was unaltered in PTbCA mice (15 days old; $n = 16$). (F and G) Static histomorphometric analysis of the femurs showed decreased osteoclast surface (Oc.S/BS) and numbers (Oc.N/B.Ar) (F) but unaltered osteoblast surface (Ob.S/BS) and numbers (Ob.N/B.Ar) (G) in PTbCA mice (15 days old; male; $n = 6$). B.Ar, bone area. (H) Dynamic histomorphometric analysis with double calcein labeling (2 months old; male; $n = 3$). (Top) Representative images of the femoral sections illustrating that the distances between the two calcein labels were similar in PTbCA mice and in the controls. Scale bar, 10 μm. (Bottom) Quantification of bone formation rate (BFR/BS) and mineral apposition rate (MAR). (I) Summary of the bone phenotype in the mouse models that harbor β-catenin constitutive activation driven by different cre drivers targeting different stages of osteoclastogenesis. The results are shown as the percent changes in the mutants compared with littermate controls (3 months old; male; $n = 4$ to 6; $P < 0.05$). The parameters include tibial trabecular BV/TV ratio, serum CTX-1 and osteocalcin, and osteoclast number (Oc.N) per well in a bone marrow osteoclast differentiation assay. *, $P < 0.05$; **, $P < 0.01$; ***, $P < 0.005$; ****, $P < 0.001$; ******, $P < 0.0001$; n.s., nonsignificant ($P > 0.05$).

bone, the cortical bone, and the whole tibia (http://www4.utsouthwestern.edu/wanlab/publications.htm). ELISA analyses revealed that the bone resorption marker CTX-1 was significantly reduced by 51% (Fig. 1D), while the bone formation marker osteocalcin was unaltered at P15 (Fig. 1E). Consistently, static histomorphometry showed that the osteoclast surface and numbers were decreased by 53% and 73%, respectively (Fig. 1F), while the osteoblast surface and numbers were unaltered (Fig. 1G). In addition, dynamic histomorphometry using double calcein labeling showed that the bone formation rate and mineral apposition rate were unaltered in the PTbCA mice (Fig. 1H). Together, these data indicate that β-catenin constitutive activation in the osteoclast lineage causes severe osteopetrosis due to diminished osteoclast numbers and bone resorption.

To examine the effect of adult-onset β-catenin activation, we treated PTbCA mutants and controls with Dox from E0 to P30 to turn off bCA and bypass development and then turned on bCA by removing Dox for 9 months (http://www4.utsouthwestern.edu/wanlab/publications.htm). These PTbCA mice also exhibited severely increased bone mass (http://www4.utsouthwestern.edu/wanlab/publications.htm), indicating that adult-onset β-catenin constitutive activation is sufficient to cause osteopetrosis. Thus, β-catenin in the osteoclast lineage is also a potent regulator of bone turnover in adulthood that is independent of its effects on development.

The abnormal osseous environment in osteopetrotic mice often shifts hematopoiesis from the bone marrow to the spleen (34, 37). Consistently, the PTbCA mice also developed extramedullary hematopoiesis that progressed with age. The number of bone marrow cells became significantly less than in the controls at ~4 months and diminished to zero at 10 months, which was compensated for by a gradual increase in splenocytes (http://www4.utsouthwestern.edu/wanlab/publications.htm).

To test whether the osteoclast defects resulted from altered RANKL or OPG levels, we measured their mRNA expression in whole tibiae. The RANKL/OPG ratio was not significantly altered in the PTbCA mutants, nor was the expression of the receptor of RANKL (RANK) or M-CSF (M-CSFR) (http://www4.utsouthwestern.edu/wanlab/publications.htm). These results indicate that the decreased osteoclast numbers and resorption are caused by an intrinsic defect in osteoclast differentiation.

As complementary approaches to investigate the osteoclast-autonomous effects of β-catenin constitutive activation, we bred $Catnb^{+/lox(ex3)}$ mice with Tie2-cre, Lyz-cre, or Ctsk-cre mice to generate Tie2-bCA, Lyz-bCA, and Ctsk-bCA mice, respectively. As summarized in Fig. 1I, Tie2-bCA mice were embryonic lethal, likely due to the targeting of all other hematopoietic lineages and endothelial cells besides osteoclasts (7, 37). Importantly, both Lyz-bCA and Ctsk-bCA mice also exhibited an increased BV/TV ratio and decreased bone resorption, yet unaltered bone formation (Fig. 1I). Together, these results strongly support the notion that β-catenin constitutive activation in the osteoclast lineage results in osteopetrosis.

β-Catenin constitutive activation blocks osteoclast differentiation and sustains precursor proliferation. To investigate the effects of β-catenin constitutive activation on osteoclast differentiation, we employed an *in vitro* system. We purified hematopoietic bone marrow (BM) cells with a 40-μm cell strainer to remove mesenchymal cells, allowing the assessment of osteoclast-autonomous defects (http://www4.utsouthwestern.edu/wanlab/publications.htm). BM cells from P15 PTbCA mutants or controls were differentiated with M-CSF and RANKL, with or without BRL (Fig. 2A). In the control cultures, the formation of multinucleated $TRAP^+$ mature osteoclasts was triggered by RANKL and further stimulated by BRL. In contrast, RANKL and BRL failed to induce osteoclast formation in the PTbCA mutant cultures (Fig. 2B). Consistently, the induction of key transcription factors (Fig. 2C) and osteoclast function genes (Fig. 2D) was severely blunted. Similar results were observed in splenocyte osteoclast differentiation cultures (http://www4.utsouthwestern.edu/wanlab/publications.htm). Furthermore, osteoclast differentiation was also significantly diminished for the BM cells from Lyz-bCA mice and Ctsk-bCA mice compared with their controls (Fig. 1I). These results indicate that β-catenin constitutive activation leads to a cell-autonomous blockade in osteoclastogenesis.

We hypothesized that β-catenin constitutive activation prevented the RANKL-induced proliferation-to-differentiation switch; thus, we tested whether it increased osteoclast precursor proliferation *in vivo* and *in vitro*. First, we examined osteoclast precursors *in vivo* using the PPARγ-tTA TRE-H2BGFP reporter mice, which labeled osteoclast progenitors and precursors as GFP^+ bone marrow cells. We bred PTbCA mice with TRE-H2BGFP (THG) mice (14c, 36a) to generate PTbCA-THG mutants or PTctrl-THG controls (Fig. 2E). Bone marrow cells were isolated from these mice or GFP^- control mice and stained with an antibody against the progenitor cell marker c-Kit or an isotype control. FACS analysis revealed that the total GFP^+ population was increased by 2.4-fold in PTbCA-THG mutants compared to PTctrl-THG controls (Fig. 2F). Moreover, both osteoclast progenitors ($GFP^+/cKit^+$) and osteoclast precursors ($GFP^+/cKit^-$) were increased, by 2.9- and 2.3-fold, respectively (Fig. 2F).

Second, we compared osteoclast precursor proliferation *in vitro*. Bone marrow cells were cultured with M-CSF for 3 days and then M-CSF starved for 6 h to synchronize the cell cycle before being restimulated with M-CSF for 4 h to induce S phase. Proliferation was quantified as BrdU incorporation during the M-CSF restimulation (2) (Fig. 2G, left). The results showed that osteoclast precursor proliferation was increased by 2.5-fold in the PTbCA cultures compared to the control cultures (Fig. 2G, right). These data indicate that β-catenin constitutive activation in the osteoclast lineage blocks osteoclast differentiation by sustaining osteoclast precursor proliferation, thus impairing the proliferation-to-differentiation switch.

β-Catenin heterozygosity in the osteoclast lineage causes osteoporosis by accelerating osteoclast differentiation. To further investigate the physiological functions of β-catenin in the osteoclast lineage, we next relied on a loss-of-function approach. Mice in which *loxP* sites had been introduced 5′ of exon 2 and 3′ of exon 6 of β-catenin ($\beta\text{-catenin}^{fl/fl}$) have been generated previously to achieve conditional β-catenin deletion (4). We bred $\beta\text{-catenin}^{fl/fl}$ mice with PPARγ-tTA TRE-cre mice to generate PPARγ-tTA TRE-cre $\beta\text{-catenin}^{fl/+}$ heterozygous mice (PTbHet) and PPARγ-tTA TRE-cre $\beta\text{-catenin}^{fl/fl}$ knockout (KO) mice (PTbKO) (Fig. 3A).

Analysis of the PTbHet mice revealed that β-catenin heterozygosity in the osteoclast lineage caused osteoporosis, an

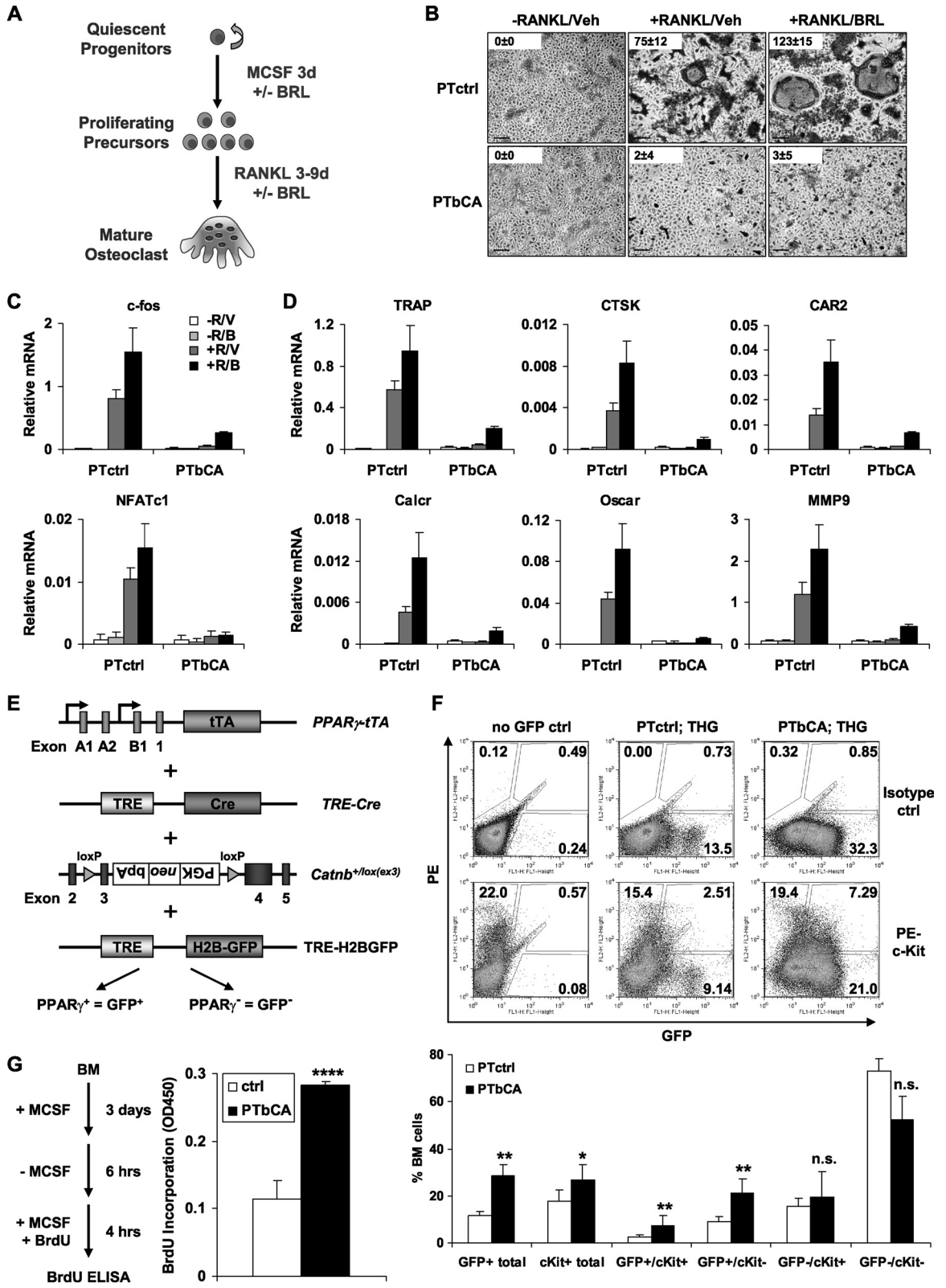

FIG. 2. β-Catenin constitutive activation blocks osteoclast differentiation and sustains osteoclast precursor proliferation. (A) Schematic diagram illustrating the osteoclast differentiation assay. (B) Representative images of TRAP-stained osteoclast differentiation cultures. Bone marrow cells were isolated from PTbCA mutants or littermate controls (15 days old; $n = 6$). Mature osteoclasts were identified as multinucleated $TRAP^+$ (purple) cells; the osteoclast number/well was determined and is shown as the average ± SD. Scale bar, 25 μm. Veh, vehicle. (C and D) RANKL-induced and BRL-stimulated induction of transcription factors (C) and osteoclast functional genes (D) was impaired in PTbCA cultures ($n = 6$). R, RANKL; V, vehicle; B, BRL. The error bars indicate SD. (E) Diagram of PPARγ-tTA TRE-Cre $Catnb^{+/lox(ex3)}$ TRE-H2BGFP

opposite phenotype from osteopetrosis. μCT imaging showed that 6-month-old PTbHet mice exhibited significantly reduced trabecular bone compared to PTctrl mice (Fig. 3B), with a smaller BV/TV ratio (−67%); less BS (−59%), Tb.N (−48%), and Tb.Th (−40%); and a greater BS/BV ratio (+50%) and more Tb.Sp (+94%) (Fig. 3C). Consistently, the BV/TV ratios of the cortical bone and the whole tibia were also decreased (Fig. 3C). The bone loss in PTbHet mice resulted from increased bone resorption marker (Fig. 3D) and osteoclast surface/numbers (Fig. 3E) but unaltered bone formation marker (Fig. 3F), osteoblast surface/numbers (Fig. 3G), and bone formation/mineral apposition rates (Fig. 3H).

An *in vitro* bone marrow differentiation assay illustrated that PTbHet cultures developed more and larger mature osteoclasts than PTctrl cultures (Fig. 3I), which was confirmed by the higher induction rate of osteoclast markers by RANKL and BRL (Fig. 3J). Moreover, *in vitro* osteoclast precursor proliferation was markedly decreased in the PTbHet cultures (Fig. 3K). To determine the effect of β-catenin heterozygosity on osteoclast precursors *in vivo*, we bred PTbHet mice with THG reporter mice. FACS analysis showed that the percentage of osteoclast precursors (GFP^+ cells) in the bone marrow was significantly reduced in the PTbHet-THG mice compared with the PTctrl-THG mice (Fig. 3L). These results indicate that β-catenin dosage reduction in the osteoclast lineage by heterozygosity accelerates the proliferation-to-differentiation switch and enhances osteoclastogenesis.

β-Catenin deletion in the osteoclast lineage causes osteopetrosis by preventing osteoclast precursor proliferation. Provocatively, the PTbKO mice exhibited osteopetrosis. μCT imaging showed that 6-month-old PTbKO mice displayed significantly more trabecular bone than PTctrl mice (Fig. 3B), with a greater BV/TV ratio (+106%) and more BS (+65%), Tb.N (+53%), and Tb.Th (+33%), accompanied by a smaller BS/BV ratio (−33%) and less Tb.Sp (−62%) (Fig. 3C). The BV/TV ratio of the cortical bone and the whole tibia was also increased (http://www4.utsouthwestern.edu/wanlab/publications.htm). CTX-1 and osteoclast surface/numbers were significantly reduced (Fig. 3D and E), while osteocalcin, osteoblast surface/numbers, and bone formation/mineral apposition rates were unaltered (Fig. 3F to H). This is in line with the fact that β-catenin was efficiently deleted in osteoclasts, but not in osteoblasts (http://www4.utsouthwestern.edu/wanlab/publications.htm). As is often seen in osteopetrotic mice, PTbKO mice also displayed extramedullary hematopoiesis (http://www4.utsouthwestern.edu/wanlab/publications.htm).

An *in vitro* differentiation assay showed that β-catenin deletion impaired osteoclastogenesis (Fig. 3I) and osteoclast marker induction (Fig. 3J). Moreover, *in vitro* osteoclast precursor proliferation was markedly decreased in the PTbKO cultures compared to PTctrl or PTbHet cultures (Fig. 3K). To determine the effect of β-catenin deletion on osteoclast precursors *in vivo*, we bred PTbKO mice with THG reporter mice. FACS analysis showed that the percentage of osteoclast precursors (GFP^+ cells) in the bone marrow was significantly reduced in the PTbKO-THG mice compared with PTctrl-THG or PTbHet-THG mice (Fig. 3L). The simultaneous blockade of both precursor proliferation and osteoclast differentiation suggested that β-catenin deletion impairs the quiescence-to-proliferation switch of the osteoclast progenitors.

As complementary approaches to investigate osteoclast-autonomous regulation by β-catenin loss-of-function *in vivo*, we also assessed the effects of Tie2-cre-mediated β-catenin deletion in hemangioblast stem cells, Lyz-Cre-mediated β-catenin deletion in macrophage precursors, and Ctsk-cre-mediated β-catenin deletion in preosteoclasts and mature osteoclasts. Tie2-bKO mice were born at below a Mendelian ratio (8% rather than 25%), indicating partial embryonic lethality. Nonetheless, Tie2-bKO mice also exhibited osteopetrosis while Tie2-bHet mice also exhibited osteoporosis due to osteoclast defects, similar to PTbKO and PTbHet mice, respectively (Fig. 3M). Furthermore, both Lyz-bKO and Ctsk-bKO mice displayed osteoporosis due to increased bone resorption, and Lyz-bHet and Ctsk-bHet mice exhibited an intermediate bone loss phenotype (Fig. 3M). Together, these gain- and loss-of-function genetic models based on different cre drivers all strongly support the cell-autonomous and dosage-dependent regulation of osteoclastogenesis by β-catenin: a minimum threshold of β-catenin is required for the quiescence-to-proliferation switch of the osteoclast progenitors, yet above this threshold, attenuated β-catenin activity accelerates whereas elevated β-catenin activity impedes the proliferation-to-differentiation switch of the osteoclast precursors. Consequently, β-catenin constitutive activation inhibits osteoclastogenesis and β-catenin suppression in the macrophage precursors accelerates osteoclastogenesis, yet complete β-catenin deletion in the osteoclast progenitors blocks osteoclastogenesis.

Ectopic β-catenin expression or Wnt activation attenuates osteoclast differentiation. To further determine whether Wnt activation suppresses osteoclast differentiation in a cell-autonomous manner, we undertook three approaches using the *in vitro* BM differentiation assay. First, we asked whether ectopic β-catenin expression could confer an osteoclast differentiation blockade. WT BM cells were transfected with a vector control or an expression plasmid encoding either WT or constitutively active β-catenin before differentiation. In the vector-transfected control cultures, many mature osteoclasts developed after 11 days of differentiation. In contrast, the WT β-catenin-transfected cultures developed fewer and smaller osteoclasts, and the constitutively active β-catenin-transfected cultures rarely developed osteoclasts but largely remained mononuclear precursors (Fig. 4A and B). This was confirmed by the impaired osteoclast marker induction, due to β-catenin overexpression (Fig. 4C). These results showed that ectopic β-catenin expression inhibits osteoclastogenesis.

(PTbCA THG) mice. (F) The osteoclast precursor population was increased in PTbCA THG mice *in vivo* compared to littermate controls (PTctrl THG). Bone marrow cells were stained with a PE-cKit antibody or a PE-isotype control and analyzed by FACS. (Top) Representative histograms. (Bottom) Percentages of GFP^+ and c-Kit^+ cells in the bone marrow cell population ($n = 6$). (G) Bone marrow-derived osteoclast precursors from PTbCA mice showed increased proliferation in response to M-CSF *in vitro*. (Left) Schematic diagram of the proliferation assay. (Right) Quantification of cell proliferation by BrdU incorporation ($n = 6$). *, $P < 0.05$; **, $P < 0.01$; ****, $P < 0.001$; n.s., nonsignificant ($P > 0.05$).

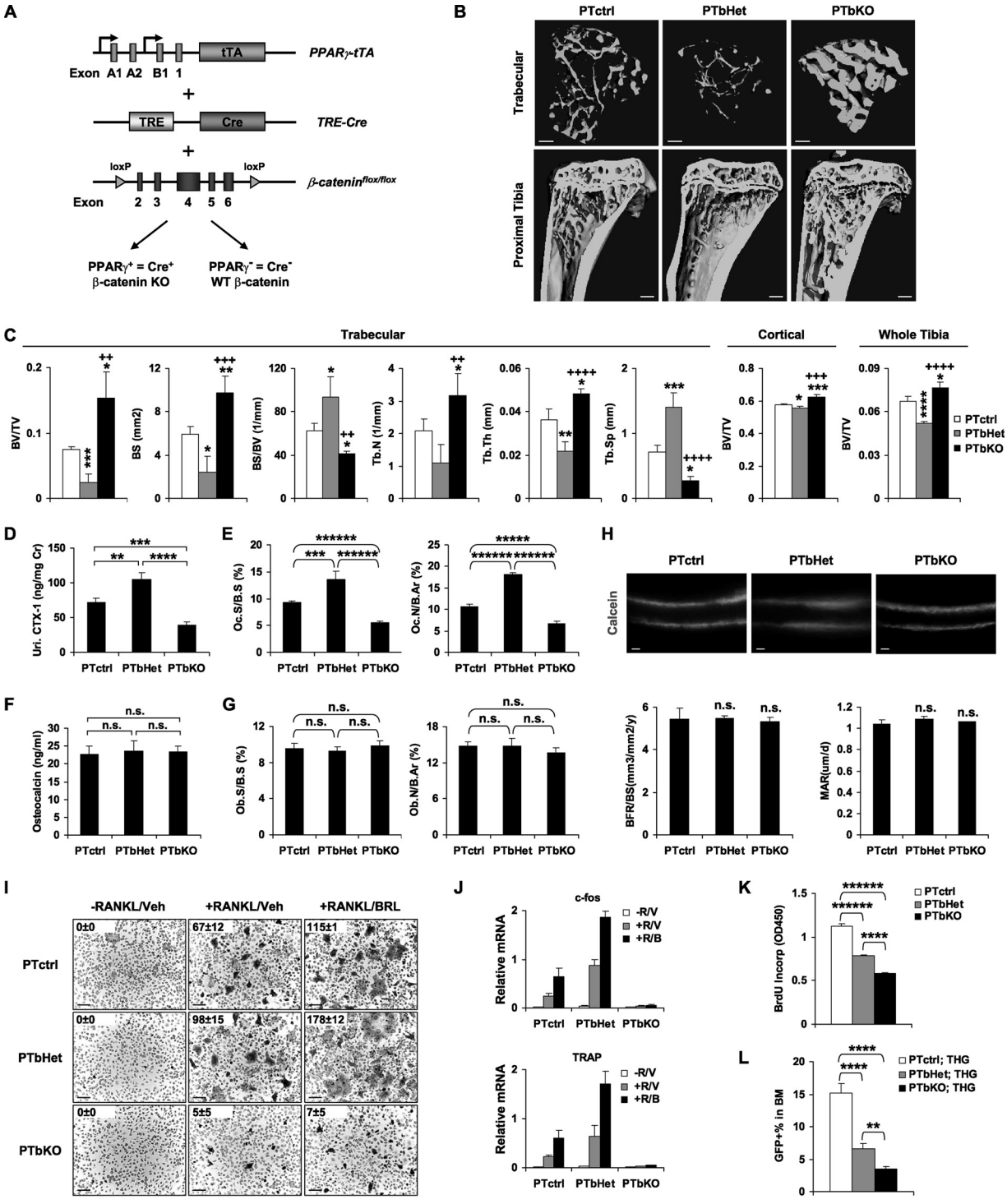

M

	Tie2-bKO	Tie2-bHet	PTbKO	PTbHet	Lyz-bKO	Lyz-bHet	Ctsk-bKO	Ctsk-bHet
BV/TV	+298%	-72%	+265%	-67%	-59%	-22%	-27%	-15%
CTX-1	-57%	+53%	-54%	+48%	+36%	+17%	+23%	+12%
Osteocalcin	N.C.	N.C.	N.C.	N.C.	N.C.	N.C.	N.C.	N.C.
OcN/Well	-85%	+197%	-94%	+215%	+143%	+54%	+68%	+24%

N.C., no significant change.

FIG. 3. β-Catenin heterozygosity enhances osteoclast differentiation, but β-catenin deletion suppresses osteoclast precursor proliferation. (A) Schematic diagram of the PPARγ-tTA TRE-cre β-catenin$^{floxed/floxed}$ (PTbKO) mice. (B and C) μCT analysis of the tibiae from PTbHet, PTbKO, or PTctrl mice (6 months old; male; $n = 5$). (B) Representative images of the trabecular bone of the tibial metaphysis (top; scale bars,

Second, we asked whether Wnt activation by GSK3β inhibition could suppress osteoclast differentiation. The GSK3β inhibitor LiCl, but not the inactive control NaCl, attenuated osteoclast differentiation (Fig. 4D and E) and osteoclast marker induction (Fig. 4F). Similar results were observed using another GSK3β inhibitor, BIO (29). BIO dose-dependently suppressed osteoclast differentiation (Fig. 4G and H) and osteoclast marker induction (Fig. 4I), whereas the inactive control metBIO (29) had no effect (Fig. 4G, H, and J). These results showed that GSK3β inhibition suppresses osteoclastogenesis.

Third, we asked whether exogenous Wnt agonist could inhibit osteoclast differentiation. The results showed that Wnt3A treatment also dose-dependently attenuated osteoclast differentiation (Fig. 4K and L). Interestingly, Western blot analyses (Fig. 4M) revealed that β-catenin protein was highly expressed in the proliferating precursors (lane 1) but downregulated upon RANKL treatment (lane 2) and further suppressed by BRL (lane 5), and Wnt3A treatment dose-dependently blocked this β-catenin protein downregulation in response to RANKL and BRL. Together, these results further illustrated that activation of Wnt/β-catenin signaling attenuates osteoclastogenesis in a cell-autonomous manner.

Biochemical Wnt inhibition enhances osteoclast differentiation. Complementary to the genetic strategy, we employed a biochemical approach to further investigate the effects of Wnt inhibition on osteoclastogenesis. Bone marrow differentiation cultures were cotreated with the IWR compound (inhibitors of Wnt response, i.e., IWRendo), which abrogates Axin degradation, or the inactive control IWRexo at increasing doses (5). In the absence of IWR, mature osteoclasts, which normally take 10 days to appear, rarely formed after 6 days; in contrast, in the presence of IWR, mature osteoclasts developed precociously, with a dose-dependent increase in number and size, whereas the IWRexo inactive control had no effect (Fig. 5A and B). Consistently, the expression of osteoclast markers was also dose-dependently elevated by IWR, normalized by the IWRexo control (Fig. 5C). The accelerated osteoclast differentiation correlated with dose-dependently decreased precursor proliferation by IWR, but not the IWRexo control (Fig. 5D). As a result, osteoclastogenesis was enhanced by IWR, with the peak induction at 2 to 4 μM (Fig. 5). Interestingly, a higher dose of IWR (10 μM) attenuated this stimulating effect (Fig. 5A to C). This was not due to any toxicity, because the IWRexo control did not decrease cell proliferation at 10 μM (Fig. 5D). These data are consistent with the *in vivo* observation that β-catenin heterozygosity promoted bone resorption, whereas β-catenin deletion suppressed bone resorption (Fig. 3). In summary, these results provide further evidence that Wnt/β-catenin signaling regulates osteoclastogenesis in a cell-autonomous and dosage-dependent manner.

Biphasic regulation of β-catenin and cyclin D1 during osteoclastogenesis. To determine the molecular mechanisms by which β-catenin regulates osteoclastogenesis, we first examined β-catenin protein levels during a time course of osteoclast differentiation. β-Catenin protein was induced upon M-CSF stimulation and highly expressed in the proliferating osteoclast precursors (day 3); however, it was downregulated upon RANKL treatment and further suppressed by BRL (Fig. 6A). The cyclin D1 gene is a well-known β-catenin target gene that mediates its proliferation-enhancing effect (32). Cyclin D1 mRNA exhibited a biphasic pattern similar to that of β-catenin protein during osteoclastogenesis (Fig. 6B), and so did cyclin D1 protein (Fig. 6A). Interestingly, BRL attenuated both β-catenin and cyclin D1 expression, which was consistent with its pro-osteoclastogenic effect (Fig. 6A and B). These results indicate that β-catenin and cyclin D1 are induced in response to M-CSF to promote the quiescence-to-proliferation switch in the osteoclast progenitors but are downregulated in response to RANKL to permit the proliferation-to-differentiation switch in the osteoclast precursors.

β-Catenin stimulates GATA2/Evi1 expression but blocks c-Jun activation. The transcription factor GATA2 is required to generate osteoclast progenitors (36, 39). We found that GATA2 mRNA was highly expressed in osteoclast progenitors and precursors on day 1 but downregulated during differentiation (Fig. 6C). Western blot analysis showed that β-catenin protein was downregulated by RANKL and further suppressed by BRL in the PTctrl cultures on day 6 but remained constitutively high in the PTbCA cultures (Fig. 6D). As a result, GATA2 mRNA expression was significantly elevated in the PTbCA cultures compared with controls (Fig. 6E). The oncogenic transcription factor Evi1 (ecotropic viral integration site 1) is required for GATA2 activation and hematopoietic pro-

10 μm) and the entire proximal tibia (bottom; scale bars, 1 mm). (C) Quantification of trabecular bone volume and architecture. The asterisks indicate the *P* value comparing PTctrl and mutant (PTbHet or PTbKO) mice; the pluses indicate the *P* value comparing PTbKO and PTbHet mice. The error bars indicate SD. (D) Urinary CTX-1 (normalized to creatinine) was increased in PTbHet mice but decreased in PTbKO mice compared with littermate controls ($n = 5$). (E) Static histomorphometry showed that osteoclast surface and numbers were increased in the PTbHet mice but decreased in the PTbKO mice ($n = 5$). (F) Serum osteocalcin was unaltered in PTbHet or PTbKO mice ($n = 5$). (G) Static histomorphometry showed that osteoblast surface and numbers were unaltered ($n = 5$). (H) Dynamic histomorphometry showed unaltered bone formation rate (BFR) and mineral apposition rate (MAR) ($n = 3$). (I) *In vitro* bone marrow osteoclast differentiation was enhanced for PTbHet mice but suppressed for PTbKO mice ($n = 3$). Mature osteoclasts were identified as multinucleated $TRAP^+$ (purple) cells; the osteoclast number/well was determined and is shown as the average ± SD. Scale bar, 25 μm. (J) RANKL-induced and BRL-stimulated induction of transcription factor (c-fos) and osteoclast functional gene (TRAP) ($n = 3$). R, RANKL; V, vehicle; B, BRL. (K) Bone marrow-derived osteoclast precursors from PTbHet and PTbKO mice showed decreased proliferation in response to M-CSF *in vitro* ($n = 3$). (L) Percentage of osteoclast precursors (GFP^+) in the bone marrow (BM) was decreased in PTbHet and PTbKO TRE-H2BGFP (THG) reporter mice compared with controls *in vivo* ($n = 3$). (M) Summary of the bone phenotype in the mouse models that harbor β-catenin heterozygosity or deletion driven by different cre drivers targeting different stages of osteoclastogenesis. The results are shown as the percent changes in the Het or KO mutants compared with littermate controls (3 months old; male; $n = 4$ to 6; $P < 0.05$). Parameters include tibial trabecular BV/TV ratio, serum CTX-1 and osteocalcin, and osteoclast number (Oc.N) per well in a bone marrow osteoclast differentiation assay. *, $P < 0.05$; ** or ++, $P < 0.01$; *** or +++, $P < 0.005$; **** or ++++, $P < 0.001$; *****, $P < 0.0005$; ******, $P < 0.0001$; n.s., nonsignificant ($P > 0.05$).

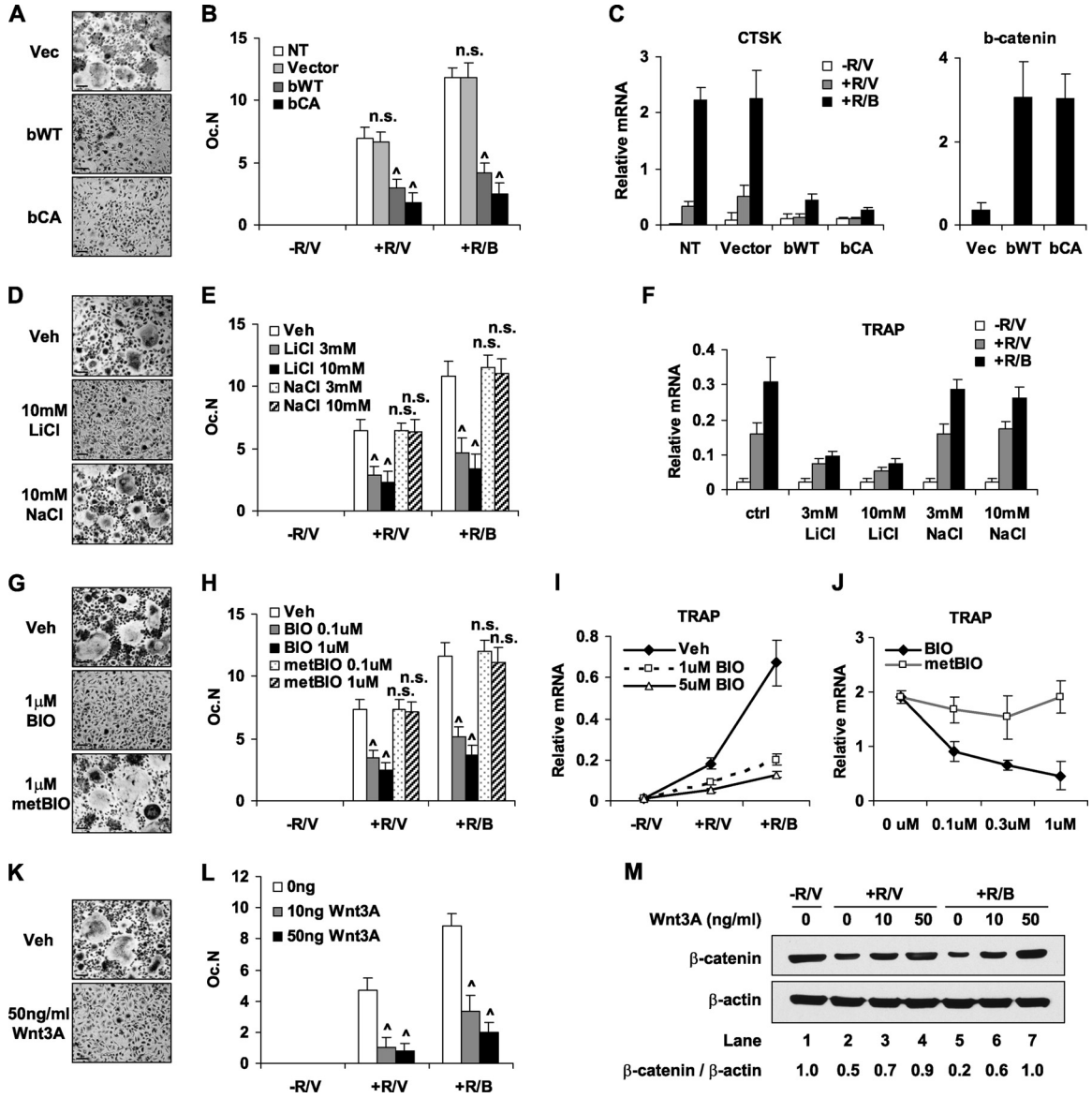

FIG. 4. Ectopic β-catenin expression or biochemical Wnt activation attenuates osteoclast differentiation. (A to C) Ectopic overexpression of wild-type β-catenin (bWT) or a constitutively active β-catenin mutant (bCA) attenuated osteoclast differentiation. Bone marrow cells were nontransfected (NT) or transfected with a β-catenin plasmid or a vector (Vec) control before RANKL treatment. (A) Representative images of TRAP-stained osteoclast differentiation cultures. Scale bars, 25 μm. (B) Quantification of the number of multinucleated (>3 nuclei) $TRAP^+$ mature osteoclasts ($n = 6$). The error bars indicate SD. (C) Expression of a representative osteoclast marker (Ctsk) and β-catenin ($n = 3$). (D to G) GSK3β inhibition by LiCl attenuated osteoclast differentiation. Bone marrow cells were treated with LiCl or an inactive control, NaCl, at the indicated concentrations. (D) Representative images of TRAP-stained osteoclast differentiation cultures. Scale bars, 25 μm. (E) Quantification of multinucleated (>3 nuclei) $TRAP^+$ mature osteoclasts ($n = 6$). (F) Expression of a representative osteoclast function gene (TRAP) ($n = 3$). (G to J) GSK3β inhibition by BIO attenuated osteoclast differentiation. Bone marrow cells were treated with BIO or an inactive control, metBIO, at the indicated concentrations. (G) Representative images of TRAP-stained osteoclast differentiation cultures. Scale bars, 25 μm. (H) Quantification of multinucleated (>3 nuclei) $TRAP^+$ mature osteoclasts ($n = 6$). (I and J) Expression of a representative osteoclast function gene was suppressed by BIO in a dose-dependent manner (I), but not by the inactive control metBIO (J) ($n = 3$). (K to M) The Wnt agonist Wnt3A attenuated osteoclast differentiation. Bone marrow cells were treated with Wnt3A or vehicle control at the indicated concentrations. (K) Representative images of TRAP-stained osteoclast differentiation cultures. Scale bars, 25 μm. (L) Quantification of multinucleated (>3 nuclei) $TRAP^+$ mature osteoclasts ($n = 6$). (M) β-Catenin downregulation by RANKL and BRL was abolished by Wnt3A in a dose-dependent manner. Whole-cell extract was collected after 6 days of differentiation and analyzed by Western blotting. The results were quantified as the β-catenin/β-actin ratio. ^, $P < 0.0001$; n.s, nonsignificant ($P > 0.05$).

genitor proliferation (40a). Evi1 expression was also increased by 50- to100-fold in the PTbCA cultures compared with the controls (Fig. 6F). In contrast, the expression of PU.1, another transcription factor critical for myeloid development, was not affected (Fig. 6G). Consistently, the GSK3β inhibitor LiCl, but not the inactive control NaCl, also significantly increased GATA2 and Evi1 expression (Fig. 6H). Furthermore, siRNA-mediated knockdown of GATA2 or Evi1 partially rescued the

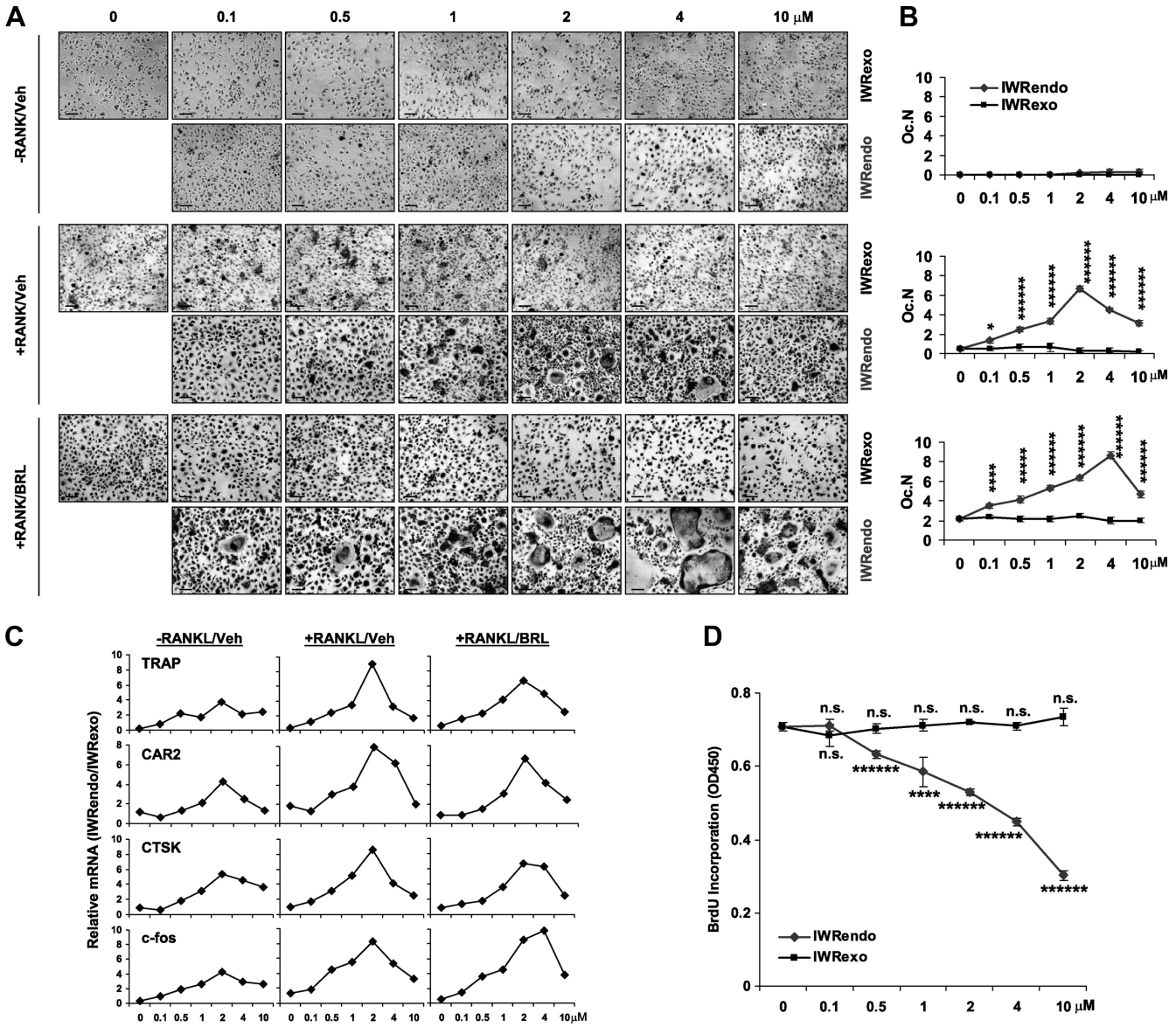

FIG. 5. Biochemical Wnt inhibition enhances osteoclast differentiation. (A to C) Bone marrow osteoclast differentiation cultures were treated with the Wnt inhibitor IWRendo or an inactive control, IWRexo, at the indicated concentrations in the presence or absence of RANKL, with or without BRL. Osteoclast formation was analyzed 6 days after differentiation (3 days after RANKL addition). (A) Representative images of TRAP-stained osteoclast differentiation cultures. Scale bars, 25 μm. (B) Quantification of multinucleated (>3 nuclei) $TRAP^+$ mature osteoclasts ($n = 6$). The error bars indicate SD. (C) Relative mRNA expression of osteoclast marker genes in the differentiation cultures treated with IWRendo, normalized by that treated with the IWRexo inactive control ($n = 6$). (D) Proliferation of bone marrow-derived osteoclast precursors in response to M-CSF was inhibited by IWRendo, but not by the IWRexo inactive control, in a dose-dependent manner ($n = 6$). *, $P < 0.05$; ****, $P < 0.001$; *****, $P < 0.0005$; ******, $P < 0.0001$; n.s., nonsignificant ($P > 0.05$).

osteoclast differentiation blockade in the PTbCA cultures (Fig. 6I). These results indicate that β-catenin activation increases GATA2 and Evi1 expression, thereby sustaining osteoclast precursor proliferation, and RANKL-induced and BRL-stimulated β-catenin downregulation is required for GATA2 and Evi1 suppression.

We next examined the effects of β-catenin activation on RANKL signaling. RANKL-induced and BRL-stimulated c-Jun phosphorylation was abolished in the PTbCA cultures, while IκBα degradation was unaffected, suggesting that β-catenin activation blocks osteoclast differentiation by inhibiting c-Jun activity (Fig. 7A). Consistently, the GSK3β inhibitor LiCl, but not the inactive control NaCl, also specifically suppressed RANKL- and BRL-induced c-Jun phosphorylation without affecting IκBα degradation (Fig. 7B). We next tested whether ectopic c-Jun activation could rescue the osteoclast differentiation blockade in the PTbCA cultures. Bone marrow cells from PTbCA mice were transfected with a vector control or an expression plasmid encoding either WT c-Jun (JunWT) or $c\text{-}Jun^{Ser63/73Asp}$ (JunS63/73D), a constitutively active mutant in which serines 63 and 73 were mutated to aspartic acid (a phosphormimetic mutation) (3, 25). The results showed that

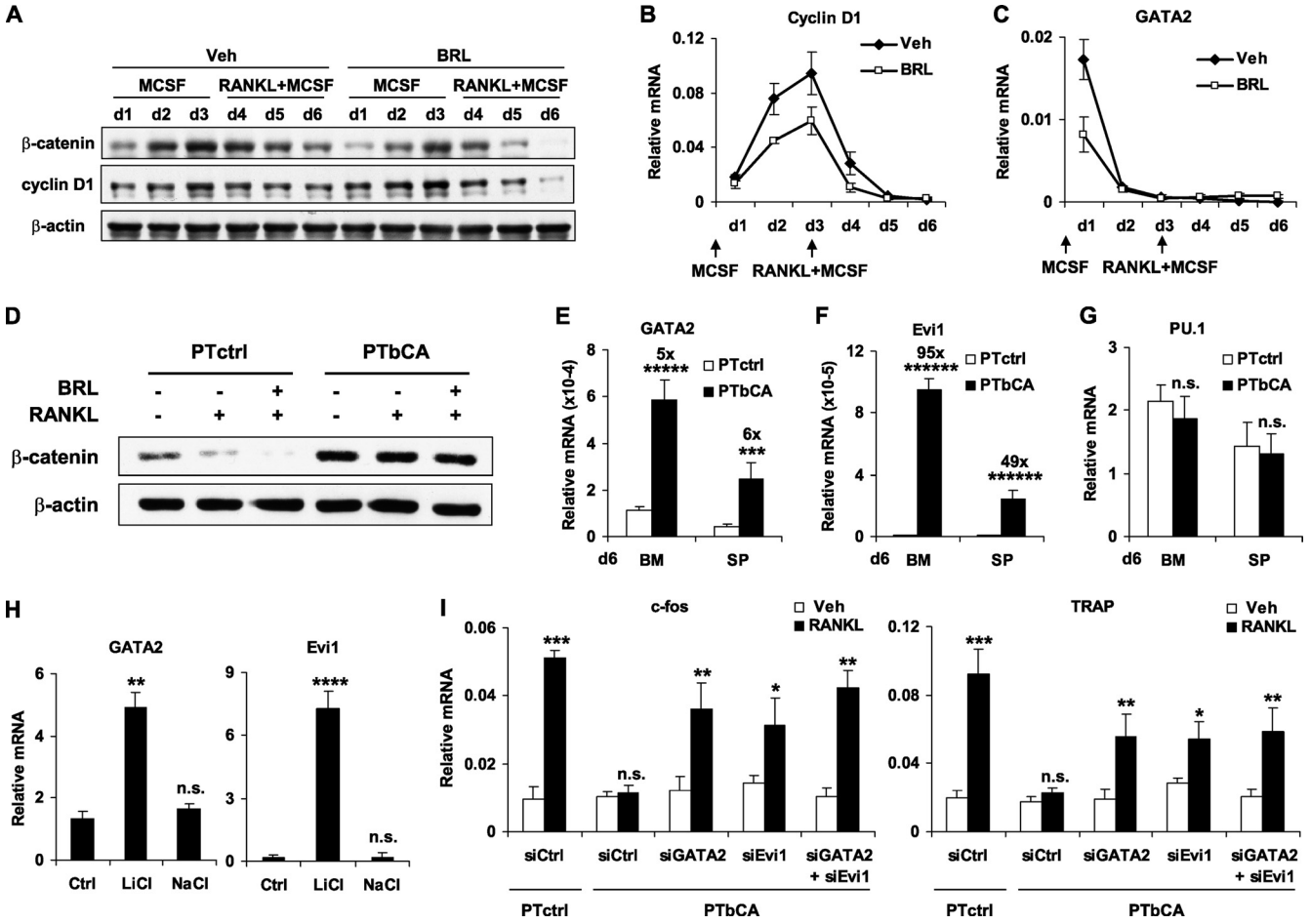

FIG. 6. β-Catenin stimulates GATA2 and Evi1 expression. (A to C) Time course expression analyses of *in vitro* bone marrow osteoclast differentiation ($n = 3$). β-Catenin and cyclin D1 protein (A), as well as cyclin D1 mRNA (B), were upregulated during M-CSF-mediated precursor proliferation but downregulated during RANKL-mediated osteoclast differentiation and further suppressed by BRL. The error bars indicate SD. d, day. (C) GATA2 mRNA expression was downregulated during osteoclastogenesis and suppressed by BRL. The arrows in panels B and C indicate that M-CSF was added on day 0 and that RANKL and M-CSF were added on day 3. (D) The β-catenin protein level was downregulated by RANKL and further reduced by BRL in control osteoclast differentiation cultures but remained constitutively high in PTbCA cultures. Whole-cell extract was collected on day 6 and analyzed by Western blotting. (E to G) Gene expression in PTbCA and control cultures on day 6 of differentiation from bone marrow (BM) or splenocytes (SP) ($n = 3$). GATA2 (E) and Evi1 (F) mRNA expression was increased in PTbCA cultures. (G) PU.1 mRNA expression was unaltered in PTbCA cultures. (H) The GSK3β inhibitor LiCl (3 mM), but not the inactive control NaCl (3 mM), increased GATA2 and Evi2 mRNA expression after 6 days of differentiation ($n = 3$). The *P* values compare treatment with the control. (I) GATA2 or Evi1 knockdown partially rescued the osteoclast differentiation blockade in PTbCA cultures. Bone marrow cells were transfected with GATA2 siRNA, Evi1 siRNA, or a control siRNA for 3 days before RANKL stimulation. Representative osteoclast marker genes were measured by RT-QPCR ($n = 3$). The *P* values compare RANKL with Veh. ⋆, $P < 0.05$; ⋆⋆, $P < 0.01$; ⋆⋆⋆, $P < 0.005$; ⋆⋆⋆⋆, $P < 0.001$; ⋆⋆⋆⋆⋆, $P < 0.0005$; ⋆⋆⋆⋆⋆⋆, $P < 0.0001$; n.s., nonsignificant ($P > 0.05$).

ectopic expression of c-Jun partially rescued the osteoclast differentiation blockade, with the JunS63/73D mutant more effective than JunWT (Fig. 6C to E). The transfection efficiency was >50% (http://www4.utsouthwestern.edu/wanlab/publications.htm), and c-Jun was significantly overexpressed (Fig. 7F). These results indicate that β-catenin activation prevents c-Jun phosphorylation, thereby blocking osteoclast differentiation, and that RANKL-induced and BRL-stimulated β-catenin downregulation is required for c-Jun activation. Together, these data provide critical molecular insights into how β-catenin employs distinct mechanisms to exert biphasic regulation of osteoclastogenesis: it promotes M-CSF-mediated precursor proliferation by inducing GATA2 and Evi1 expression, and it blocks RANKL-mediated osteoclast differentiation by impairing c-Jun activation.

DISCUSSION

In this study, we have identified the canonical Wnt/β-catenin pathway as a previously unrecognized yet critical regulator of osteoclastogenesis. β-Catenin protein is induced during the quiescence-to-proliferation switch of the osteoclast progenitors in response to M-CSF but downregulated during the proliferation-to-differentiation switch in response to RANKL (Fig. 7G). Genetically, β-catenin deletion impairs osteoclast precursor proliferation, while β-catenin constitutive activation

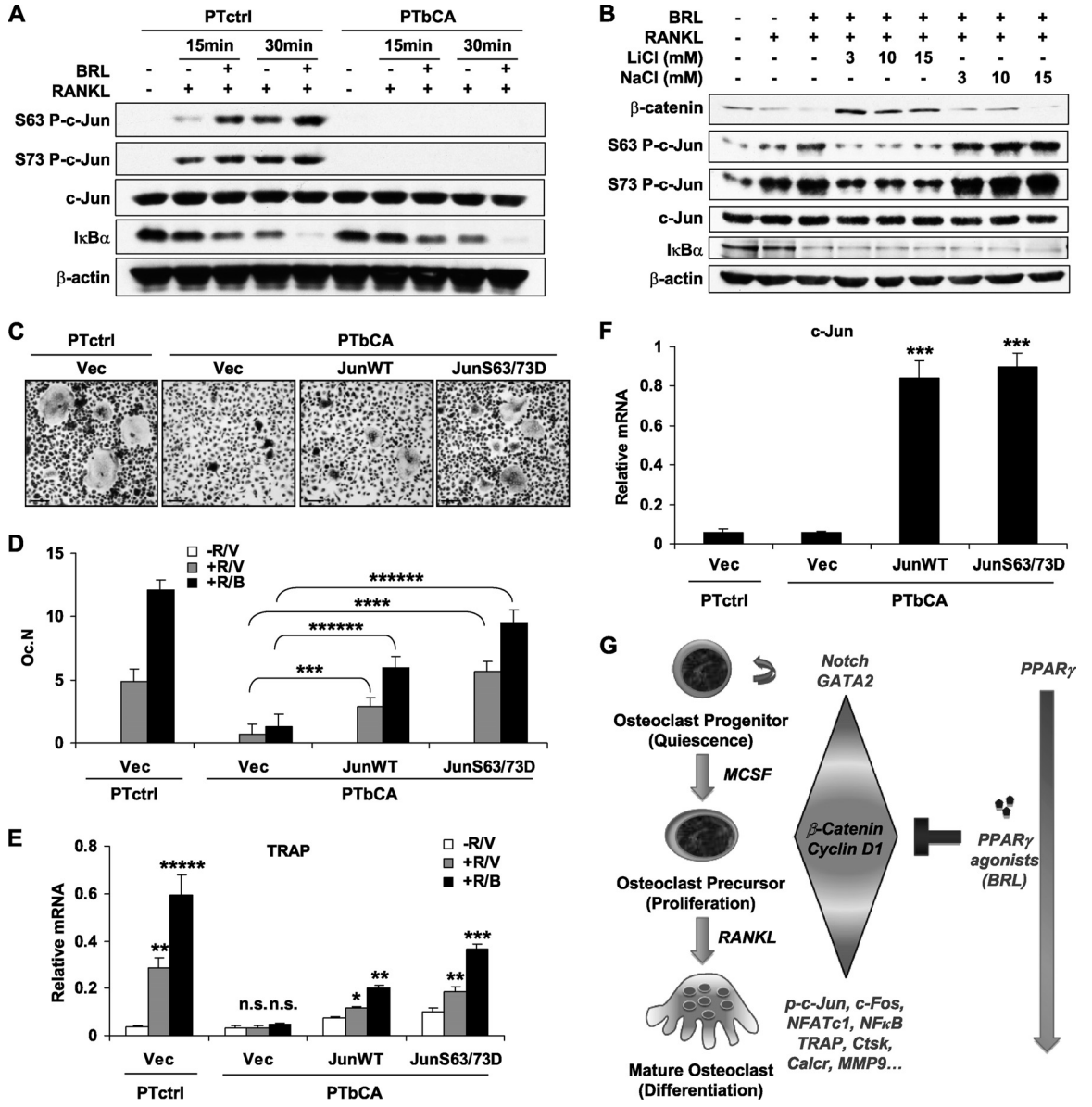

FIG. 7. β-Catenin blocks c-Jun activation. (A) RANKL-induced and BRL-stimulated c-Jun phosphorylation, but not IκBα degradation, were abolished in PTbCA cultures. Bone marrow cells from PTbCA or PTctrl mice were treated with M-CSF for 3 days in the presence or absence of BRL and then stimulated with RANKL for 15 or 30 min. Whole-cell extract was analyzed by Western blotting. (B) RANKL-induced and BRL-stimulated β-catenin downregulation and c-Jun phosphorylation, but not IκBα degradation, were abolished by the GSK3β inhibitor LiCl, but not by the inactive control, NaCl. Whole-cell extract was collected on day 6 and analyzed by Western blotting. (C to F) Ectopic overexpression of either a wild-type c-Jun (JunWT) or a constitutively active c-Jun mutant (JunS63/73D) rescued the osteoclast differentiation blockade in PTbCA cultures. Bone marrow cells were transfected with a c-Jun plasmid or a vector control (Vec) and differentiated with RANKL and M-CSF, with or without BRL. (C) Representative images of TRAP-stained osteoclast differentiation cultures. Scale bars, 25 μm. (D) Quantification of multinucleated (>3 nuclei) TRAP$^+$ mature osteoclasts ($n = 6$). The error bars indicate SD. (E) Quantification of the mRNA expression of a representative osteoclast functional gene ($n = 3$). (F) Quantification of the mRNA expression of c-Jun ($n = 3$). (G) Simplified model illustrating the biphasic and dosage-dependent regulation of osteoclastogenesis by β-catenin. β-Catenin and its cyclin D1 target gene are induced by M-CSF to promote the quiescence-to-proliferation switch but are downregulated by RANKL to permit the proliferation-to-differentiation switch. β-Catenin dosage reduction, for example, by the PPARγ agonist BRL, accelerates osteoclastogenesis. *, $P < 0.05$; **, $P < 0.01$; ***, $P < 0.005$; ****, $P < 0.001$; *****, $P < 0.0005$; ******, $P < 0.0001$; n.s., nonsignificant ($P > 0.05$).

sustains precursor proliferation, both blocking osteoclast differentiation and causing osteopetrosis. In contrast, β-catenin dosage reduction by heterozygosity enhances osteoclast differentiation and causes osteoporosis. Biochemically, β-catenin activation by GSK3β inhibitors or a Wnt ligand attenuates osteoclastogenesis, whereas β-catenin suppression by a Wnt inhibitor or a PPARγ agonist stimulates osteoclastogenesis. Mechanistically, β-catenin activation promotes precursor proliferation by elevating GATA2 and Evi1 expression and blocks osteoclast differentiation by preventing c-Jun phosphorylation.

Therefore, β-catenin exerts a biphasic regulation of osteoclastogenesis: its induction is required for M-CSF-mediated precursor proliferation, yet its degradation is required for RANKL-mediated osteoclast differentiation. Moreover, β-catenin controls osteoclast differentiation in a dosage-dependent manner: a minimum threshold of β-catenin is required for osteoclast progenitors to proliferate, yet above this threshold, β-catenin activation suppresses osteoclast differentiation, while β-catenin attenuation accelerates osteoclast differentiation.

In order to understand the full spectrum of β-catenin functions in osteoclastogenesis, it is essential to target the entire osteoclast lineage from osteoclast progenitors to mature osteoclasts. However, the intrinsic multipotent property of stem/progenitor cells renders it impossible to specifically target the osteoclast lineage. Therefore, by establishing a suite of genetic models using different cre drivers targeting different stages of osteoclastogenesis, we were able to extract the cell-autonomous regulation of osteoclastogenesis by β-catenin. The PPARγ-driven β-catenin models permit osteoclast progenitor targeting without the embryonic lethality seen in the Tie2-driven β-catenin models. Importantly, the bone phenotype in the PPARγ-driven β-catenin models was not due to any MSC or osteoblast targeting, because (i) the reported MSC-bKO mice were embryonic lethal (8) while, in contrast, the PTbKO mice were viable; (ii) the reported osteoblast-bCA mice died a few days after weaning with a BV/TV ratio of 23% (11) while, in contrast, the PTbCA mice lived for >12 months with a BV/TV ratio of >80%; (iii) osteoblast numbers and bone formation were largely unaltered in these mice. This strongly supports the notion that the bone phenotype in these mice was mainly the result of osteoclast-autonomous defects. Furthermore, although the Lyz-Cre- and Ctsk-cre-driven β-catenin models cannot target osteoclast progenitors, they permit more specific targeting to macrophage precursors and osteoclasts, respectively. The results, with Lyz-bCA and Ctsk-bCA mice exhibiting osteopetrosis while Lyz-bKO and Ctsk-bKO mice exhibited osteoporosis, confirmed that β-catenin constitutive activation inhibits osteoclastogenesis and β-catenin dosage reduction in the macrophage precursors stimulates osteoclastogenesis. However, Lyz-bKO and Ctsk-bKO mice did not reveal the critical requirement of β-catenin in the quiescence-to-proliferation switch of the osteoclast progenitors, which was uncovered in the PTbKO and Tie2-bKO mice. Therefore, these studies also highlight the inducible PPARγ-tTA-TRE-cre driver as a novel strategy for targeting osteoclast progenitors and the entire osteoclast lineage that is complementary to the existing cre drivers.

Wnt activation is a promising therapeutic strategy for treating bone diseases based on its currently known bone formation-stimulating anabolic effects. For example, a neutralizing monoclonal antibody (Scl-Ab) against the Wnt antagonist sclerostin (sost), which is secreted specifically from osteocytes (27), has been shown to markedly increase bone formation and reverse estrogen deficiency-induced bone loss (19, 23). Currently, Scl-Ab is being developed by Amgen as a new anabolic treatment for bone disorders, such as postmenopausal osteoporosis. Furthermore, a neutralizing monoclonal antibody (BHQ880) against the Wnt antagonist Dickkopf-1 (DKK-1), which is expressed predominantly in adult bone and upregulated in multiple myeloma (33), has been shown to increase bone formation in murine models of human multiple myeloma and rheumatoid arthritis (9, 10). Currently, BHQ880 is being developed by Novartis as a new approach to promote bone formation and thereby inhibit tumor-induced osteolysis. Our findings provide strong evidence that Wnt activation also inhibits osteoclast differentiation and bone resorption, illuminating a previously unrecognized additional anticatabolic benefit. Consistent with this notion, in a recent first-in-humans study, a sclerostin monoclonal antibody (AMG 785) not only increased bone formation marker but also decreased bone resorption marker in a dose-dependent manner (24). Therefore, bone-specific activators of Wnt/β-catenin signaling may promise an exciting new class of drugs that can more effectively prevent and treat skeletal fragility.

In summary, the discovery of novel roles of β-catenin in osteoclastogenesis in this study opens an exciting new path to future investigations of the ligands, receptors, signal transducers, and transcription factors that orchestrate the regulation of osteoclast physiology and pharmacology by the Wnt pathway.

ACKNOWLEDGMENTS

We thank L. Lum (University of Texas Southwestern Medical Center) for providing the IWRendo and IWRexo compounds, D. Bohmann (University of Rochester) for providing the c-Jun plasmids, C. Zhang (Texas Scottish Rite Hospital for Children) for providing the β-catenin plasmids, S. Kato (University of Tokyo) for providing the Ctsk-cre mice, L. Smith (Baylor College of Dentistry, Texas A&M University Health Sciences Center) for assistance with μCT analysis, and D. Mangelsdorf and S. Kliewer for helpful discussion.

This work was supported by the University of Texas Southwestern Medical Center Endowed Scholar Startup Fund (Y.W.), a BD Biosciences Research Grant Award (Y.W.), CPRIT (RP100841 [Y.W.]), the March of Dimes (5-FY10-1 [Y.W.]), the Welch Foundation (I-1751 [Y.W.]), NIH (R01 DK089113 [Y.W.] and R01 DK066556, R01 DK064261, and R01 DK088220 [J.M.G.]), and a predoctoral fellowship (D.Z.) from the American Heart Association South Central Affiliate. Y.W. is a Virginia Murchison Linthicum Scholar in Medical Research.

J.M.G. is a founder of Reata Pharmaceuticals. We declare that we have no financial conflict of interest.

REFERENCES

1. **Ash, P., J. F. Loutit, and K. M. Townsend.** 1980. Osteoclasts derived from haematopoietic stem cells. Nature **283:**669–670.
2. **Bai, S., et al.** 2008. NOTCH1 regulates osteoclastogenesis directly in osteoclast precursors and indirectly via osteoblast lineage cells. J. Biol. Chem. **283:**6509–6518.

2a. **Bennett, C. N., et al.** 2005. Regulation of osteoblastogenesis and bone mass by Wnt10b. Proc. Natl. Acad. Sci. U. S. A. **102:**3324–3329.

3. **Bohmann, D., and R. Tjian.** 1989. Biochemical analysis of transcriptional activation by Jun: differential activity of c- and v-Jun. Cell **59:**709–717.
4. **Brault, V., et al.** 2001. Inactivation of the beta-catenin gene by Wnt1-Cre-mediated deletion results in dramatic brain malformation and failure of craniofacial development. Development **128:**1253–1264.
5. **Chen, B., et al.** 2009. Small molecule-mediated disruption of Wnt-dependent signaling in tissue regeneration and cancer. Nat. Chem. Biol. **5:**100–107.
6. **Clausen, B. E., C. Burkhardt, W. Reith, R. Renkawitz, and I. Forster.** 1999. Conditional gene targeting in macrophages and granulocytes using LysMcre mice. Transgenic Res. **8:**265–277.
7. **Constien, R., et al.** 2001. Characterization of a novel EGFP reporter mouse to monitor Cre recombination as demonstrated by a Tie2 Cre mouse line. Genesis **30:**36–44.
8. **Day, T. F., X. Guo, L. Garrett-Beal, and Y. Yang.** 2005. Wnt/beta-catenin signaling in mesenchymal progenitors controls osteoblast and chondrocyte differentiation during vertebrate skeletogenesis. Dev. Cell **8:**739–750.
9. **Diarra, D., et al.** 2007. Dickkopf-1 is a master regulator of joint remodeling. Nat. Med. **13:**156–163.
10. **Fulciniti, M., et al.** 2009. Anti-DKK1 mAb (BHQ880) as a potential therapeutic agent for multiple myeloma. Blood **114:**371–379.
11. **Glass, D. A., II, et al.** 2005. Canonical Wnt signaling in differentiated osteoblasts controls osteoclast differentiation. Dev. Cell **8:**751–764.

12. **Harada, N., et al.** 1999. Intestinal polyposis in mice with a dominant stable mutation of the beta-catenin gene. EMBO J. **18:**5931–5942.
13. **Haynes, D. R., et al.** 2001. Osteoprotegerin and receptor activator of nuclear factor kappaB ligand (RANKL) regulate osteoclast formation by cells in the human rheumatoid arthritic joint. Rheumatology (Oxford) **40:**623–630.
13a. **Hill, T. P., D. Spater, M. M. Taketo, W. Birchmeier, and C. Hartmann.** 2005. Canonical Wnt/beta-catenin signaling prevents osteoblasts from differentiating into chondrocytes. Dev. Cell. **8:**727–738.
14. **Holmen, S. L., et al.** 2005. Essential role of beta-catenin in postnatal bone acquisition. J. Biol. Chem. **280:**21162–21168.
14a. **Hughes, D. E., et al.** 1996. Estrogen promotes apoptosis of murine osteoclasts mediated by TGF-beta. Nat. Med. **2:**1132–1136.
14b. **Kameda, T., et al.** 1997. Estrogen inhibits bone resorption by directly inducing apoptosis of the bone-resorbing osteoclasts. J Exp Med **186:**489–495.
14c. **Kanda, T., K. F. Sullivan, and G. M. Wahl.** 1998. Histone-GFP fusion protein enables sensitive analysis of chromosome dynamics in living mammalian cells. Curr. Biol. **8:**377–385.
14d. **Kang, S., et al.** 2007. Wnt signaling stimulates osteoblastogenesis of mesenchymal precursors by suppressing CCAAT/enhancer-binding protein alpha and peroxisome proliferator-activated receptor gamma. J. Biol. Chem. **282:**14515–14524.
15. **Kawano, H., et al.** 2003. Suppressive function of androgen receptor in bone resorption. Proc. Natl. Acad. Sci. U. S. A. **100:**9416–9421.
16. **Kisanuki, Y. Y., et al.** 2001. Tie2-Cre transgenic mice: a new model for endothelial cell-lineage analysis in vivo. Dev. Biol. **230:**230–242.
17. **Kong, Y. Y., et al.** 1999. Activated T cells regulate bone loss and joint destruction in adjuvant arthritis through osteoprotegerin ligand. Nature **402:**304–309.
17a. **Kousteni, S., et al.** 2002. Reversal of bone loss in mice by nongenotropic signaling of sex steroids. Science **298:**843–846.
18. **Lacey, D. L., et al.** 1998. Osteoprotegerin ligand is a cytokine that regulates osteoclast differentiation and activation. Cell **93:**165–176.
18a. **Lazarenko, O. P., et al.** 2007. Rosiglitazone induces decreases in bone mass and strength that are reminiscent of aged bone. Endocrinology **148:**2669–2680.
19. **Li, X., et al.** 2009. Sclerostin antibody treatment increases bone formation, bone mass, and bone strength in a rat model of postmenopausal osteoporosis. J. Bone Miner. Res. **24:**578–588.
20. **Logan, C. Y., and R. Nusse.** 2004. The Wnt signaling pathway in development and disease. Annu. Rev. Cell Dev. Biol. **20:**781–810.
20a. **Mundy, G. R.** 2002. Metastasis to bone: causes, consequences and therapeutic opportunities. Nat. Rev. Cancer **2:**584–593.
21. **Nakamura, T., et al.** 2007. Estrogen prevents bone loss via estrogen receptor alpha and induction of Fas ligand in osteoclasts. Cell **130:**811–823.
22. **Novack, D. V., and S. L. Teitelbaum.** 2008. The osteoclast: friend or foe? Annu. Rev. Pathol. **3:**457–484.
23. **Ominsky, M. S., et al.** 2010. Two doses of sclerostin antibody in cynomolgus monkeys increases bone formation, bone mineral density, and bone strength. J. Bone Miner. Res. **25:**948–959.
24. **Padhi, D., G. Jang, B. Stouch, L. Fang, and E. Posvar.** 2011. Single-dose, placebo-controlled, randomized study of AMG 785, a sclerostin monoclonal antibody. J. Bone Miner. Res. **26:**19–26.
25. **Papavassiliou, A. G., M. Treier, and D. Bohmann.** 1995. Intramolecular signal transduction in c-Jun. EMBO J. **14:**2014–2019.
26. **Pittenger, M. F., et al.** 1999. Multilineage potential of adult human mesenchymal stem cells. Science **284:**143–147.
27. **Poole, K. E., et al.** 2005. Sclerostin is a delayed secreted product of osteocytes that inhibits bone formation. FASEB J. **19:**1842–1844.
28. **Ricote, M., A. C. Li, T. M. Willson, C. J. Kelly, and C. K. Glass.** 1998. The peroxisome proliferator-activated receptor-gamma is a negative regulator of macrophage activation. Nature **391:**79–82.
28a. **Roodman, G. D.** 2004. Mechanisms of bone metastasis. N. Engl. J. Med. **350:**1655–1664.
29. **Sato, N., L. Meijer, L. Skaltsounis, P. Greengard, and A. H. Brivanlou.** 2004. Maintenance of pluripotency in human and mouse embryonic stem cells through activation of Wnt signaling by a pharmacological GSK-3-specific inhibitor. Nat. Med. **10:**55–63.
30. **Takada, I., A. P. Kouzmenko, and S. Kato.** 2009. Wnt and PPARgamma signaling in osteoblastogenesis and adipogenesis. Nat. Rev. Rheumatol. **5:**442–447.
31. **Tang, W., et al.** 2008. White fat progenitor cells reside in the adipose vasculature. Science **322:**583–586.
32. **Tetsu, O., and F. McCormick.** 1999. Beta-catenin regulates expression of cyclin D1 in colon carcinoma cells. Nature **398:**422–426.
33. **Tian, E., et al.** 2003. The role of the Wnt-signaling antagonist DKK1 in the development of osteolytic lesions in multiple myeloma. N. Engl. J. Med. **349:**2483–2494.
34. **Tolar, J., S. L. Teitelbaum, and P. J. Orchard.** 2004. Osteopetrosis. N. Engl. J. Med. **351:**2839–2849.
35. **Tontonoz, P., L. Nagy, J. G. Alvarez, V. A. Thomazy, and R. M. Evans.** 1998. PPARgamma promotes monocyte/macrophage differentiation and uptake of oxidized LDL. Cell **93:**241–252.
36. **Tsai, F. Y., et al.** 1994. An early haematopoietic defect in mice lacking the transcription factor GATA-2. Nature **371:**221–226.
36a. **Tumbar, T., et al.** 2004. Defining the epithelial stem cell niche in skin. Science **303:**359–363.
37. **Wan, Y., L. W. Chong, and R. M. Evans.** 2007. PPAR-gamma regulates osteoclastogenesis in mice. Nat. Med. **13:**1496–1503.
38. **Wei, W., et al.** 2010. PGC1beta mediates PPARgamma activation of osteoclastogenesis and rosiglitazone-induced bone loss. Cell Metab. **11:**503–516.
38a. **Wei, W., et al.** 2011. Osteoclast progenitors reside in the peroxisome proliferator-activated receptor γ-expressing bone marrow cell population. Mol. Cell. Biol. **31:**4692–4705.
39. **Yamane, T., et al.** 2000. Sequential requirements for SCL/tal-1, GATA-2, macrophage colony-stimulating factor, and osteoclast differentiation factor/osteoprotegerin ligand in osteoclast development. Exp. Hematol. **28:**833–840.
40. **Yasuda, H., et al.** 1998. Osteoclast differentiation factor is a ligand for osteoprotegerin/osteoclastogenesis-inhibitory factor and is identical to TRANCE/RANKL. Proc. Natl. Acad. Sci. U. S. A. **95:**3597–3602.
40a. **Yuasa, H., et al.** 2005. Oncogenic transcription factor Evi1 regulates hematopoietic stem cell proliferation through GATA-2 expression. EMBO J. **24:**1976–1987.
41. **Zhang, C., et al.** 2008. Inhibition of Wnt signaling by the osteoblast-specific transcription factor Osterix. Proc. Natl. Acad. Sci. U. S. A. **105:**6936–6941.
42. **Zinman, B., et al.** 2010. Effect of rosiglitazone, metformin, and glyburide on bone biomarkers in patients with type 2 diabetes. J. Clin. Endocrinol. Metab. **95:**134–142.